

Document downloaded from:

<http://hdl.handle.net/10251/56444>

This paper must be cited as:

Ali, M.; Ahmed, I.; Nasir, S.; Ramirez Hoyos, P.; Niemeyer, CM.; Mafe, S.; Ensinger, W. (2015). Ionic transport through chemically functionalized hydrogen peroxide-sensitive asymmetric nanopores. *ACS Applied Materials and Interfaces*. 7(35):19541-19545. doi:10.1021/acsami.5b06015.



The final publication is available at

<http://dx.doi.org/10.1021/acsami.5b06015>

Copyright American Chemical Society

Additional Information

Reversibly Functionalizable Hydrogen Peroxide-Sensitive Asymmetric Nanopores

Mubarak Ali,^{*,1,2} Ishtiaq Ahmed,³ Saima Nasir,^{1,2} Patricio Ramirez,⁴, Christof M. Niemeyer,³ Salvador Mafe,⁵ and Wolfgang Ensinger¹

¹*Department of Material- and Geo-Sciences, Materials Analysis, Technische Universität Darmstadt, D-64287 Darmstadt, Germany*

²*Materialforschung, GSI Helmholtzzentrum für Schwerionenforschung, D-64291, Darmstadt, Germany*

³*Karlsruhe Institute of Technology (KIT), Institute for Biological Interfaces (IBG-1), Hermann-von-Helmholtz-Platz, D-76344 Eggenstein-Leopoldshafen, Germany.*

⁴*Departament de Física Aplicada, Universitat Politècnica de València, E-46022 València, Spain*

⁵*Departament de Física de la Terra i Termodinàmica, Universitat de València, E-46100 Burjassot, Spain.*

ABSTRACT

We describe the fabrication of a chemical-sensitive nanofluidic device based on asymmetric nanopores whose transport characteristics can be modulated upon exposure to hydrogen peroxide (H_2O_2). We show experimentally and theoretically that the current–voltage curves provide a suitable method to monitor the change of pore surface characteristics induced by H_2O_2 in solution from the electronic readouts. We demonstrate also that the single pore characteristics can be scaled to the case of a multipore membrane whose electric outputs can be readily controlled. Because H_2O_2 is an agent significant for medical diagnostics, the results should be useful for sensing nanofluidic devices.

*Address correspondence to m.ali@gsi.de

In this letter, we describe the reversible chemical functionalization of hydrogen peroxide (H_2O_2)-sensitive asymmetric nanopores, showing experimentally and theoretically that the current-voltage (I - V) curves of a single pore provide a suitable method to monitor the solution properties from electronic readouts. We demonstrate also the scalability of the single pore characteristics to the case of a multipore membrane whose output electrical signals can be readily controlled. The reversibility of the surface functionalization process suggests the possibility of reusing the pores while the scalability paves the way to integration into functional devices through multipore membranes. Note that H_2O_2 is an agent significant for medical diagnostics¹⁻⁵ which is usually monitored by biological, chemical and electrochemical methods based on spectrometry,^{4,6} chemoluminescence,^{7,8} and amperometry.^{9,10} An alternative method is based on confining the sensing process within a single nanopore whose inner surface is functionalized, e.g., with the covalently linked enzyme horseradish peroxidase.¹¹ The changes observed in the I - V curves can then be correlated with the presence of H_2O_2 in the external solution. High sensor sensitivities can be achieved because of the small working volume and the off-the-shelf electronic equipment.¹²

The asymmetric track-etching technique¹² was employed here to fabricate the asymmetric nanopores in polyethylene terephthalate (PET) membranes of thickness 12 μm . Both single pore and multipore (10^4 pores/ cm^2) membranes were obtained by heavy ion irradiation and subsequent chemical track-etching process (see *Supporting Information* for experimental details). The resulting carboxylic acid ($-\text{COOH}$) groups were exposed on the pore surface.¹³ These groups act as starting points for the covalent attachment of different functionalities which modulate the electrochemical characteristics of the pore surface (Figure 1a-d).

To fabricate the hydrogen peroxide sensitive nanopore, we have synthesized an amine-terminated boronic ester carbamate (**6**) (BEC-NH_2) chemical compound (see *Supporting Information, SI* for detail). Briefly, the starting material 4-(4,4,5,5-tetramethyl-1,3,2-dioxaborolan-2-yl)benzylalcohol (**1**) was first synthesized in excellent yield by already reported method.¹⁴ Then, the activation of benzyl alcohol (**1**) was performed with carbonyldiimidazol (**2**) in anhydrous acetonitrile to give a stable imidazole carbamate (**3**).¹⁵ Subsequently, the reaction of *N*-*boc*-1,6-hexanediamine (**4**) with imidazole carbamate (**3**) gave *N*-*boc*-protected carbamate (**5**). The protected carbamate (**5**) was treated with trifluoroacetic acid in dichloromethane (1:3) to give the BEC-NH_2 (**6**) compound.

The covalent functionalization of the BEC–NH₂ on the pore surface was achieved through *N*-(3-dimethylaminopropyl)-*N'*-ethylcarbodiimide pentafluorophenol (EDC/PFP) coupling chemistry (Figure 1 a-b).¹⁶ Finally, the surface amine groups were converted into carboxylic acids moieties (Figure 1c-d) by reaction with succinic anhydride (SA).¹⁷

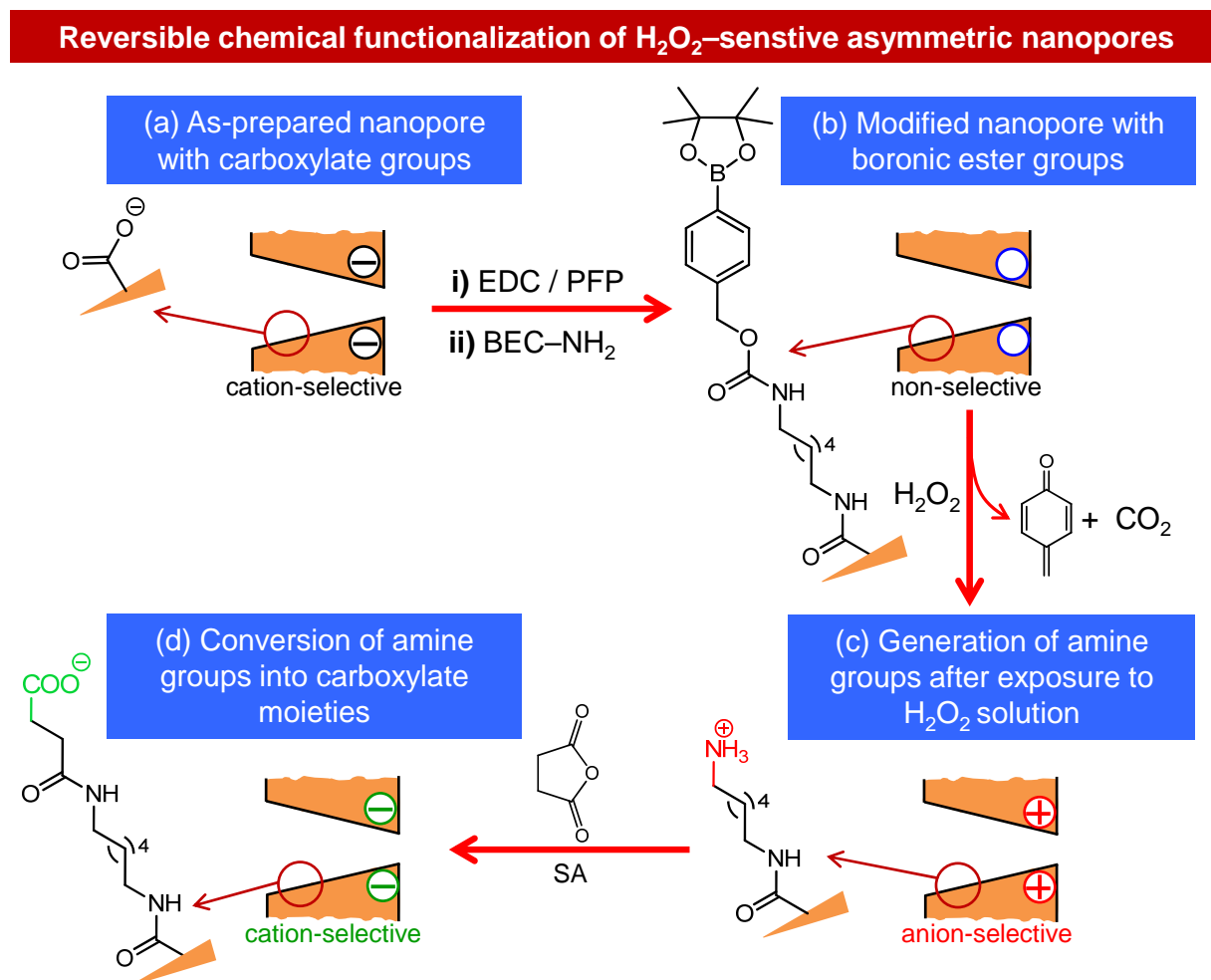


Figure 1. (a)-(b) The surface functionalization of the carboxylic acid groups with amine-terminated boronic ester carbamate (BEC-NH₂) moieties via carbodiimide coupling chemistry. (b)-(c) The H₂O₂ triggered generation of amine groups on the pore surface. (c)-(d) The conversion of surface amine groups into carboxylic acids moieties by reaction with succinic anhydride (SA).

Figure 2a shows the *I*–*V* curves of a single asymmetric nanopore before and after the functionalization of the H₂O₂ sensitive molecules on the inner pore surface (Figure 1a-b). The rectification characteristics, described by the ratio $|I(+2V)|/|I(-2V)|$ in the inset, arise from the electrostatic interaction of the asymmetrically distributed surface charge with the mobile ions in solution.¹⁴ The *I*–*V* curves were obtained under symmetrical electrolyte conditions using a non-

buffered 0.1 M KCl solution at $pH = 5.6 \pm 0.2$ in the conductivity cell. The as-prepared, unmodified asymmetric pore is cation selective (Figure 1a) and rectifies the ionic current (Figure 2a). The preferential direction of cation flow is from the narrow tip towards the wide opening.^{18,19} After modification, the anchoring of the BEC–NH₂ neutral chains having uncharged terminal boronic ester decreased the pore surface charge density, in agreement with the significant decrease observed in the pore rectification ratio, from 5.7 to 1.7.

Figure 1b-c shows the generation of amine groups upon exposing the BEC-modified pore to a solution of H₂O₂. The slightly alkaline solution of H₂O₂ can hydrolyze the arylboronic ester into a corresponding phenol.²⁰ The resulting phenolic compound further undergoes decarboxylation and 1,6-elimination reactions, leading to the generation of amine groups.²¹ H₂O₂ acts as a triggering agent which generates the amine groups on the backbone of the boronic ester carbamate chains.²¹ Figure 2b shows the I – V curves of the BEC-modified pore when exposed to a H₂O₂ solution for different times. As expected, an inversion of the ionic current rectification^{18,19} with respect to that of Figure 2a was observed due to the amine moieties on the pore surface (in our experimental conditions, the amine groups are protonated, imparting positive charge to the pore surface). This process also leads to the conversion of the inner pore environment from a hydrophobic nonconducting state to a hydrophilic conducting state.

Figure 2b suggests that the exposure time to the H₂O₂ solution was proportionally related to the generation of amine groups, which changes the pore rectification and ionic current. After 60 min of exposure time, the value of positive current was decreases while that of the negative current increased (in absolute value) compared with the reference values of the BEC-modified pore. Further increase in the exposure time enhanced the above experimental trends because of the increased pore surface charges. However, after 180 min of exposure time, no significant change in the positive and negative ion currents was observed, indicating the saturation of the surface charge.

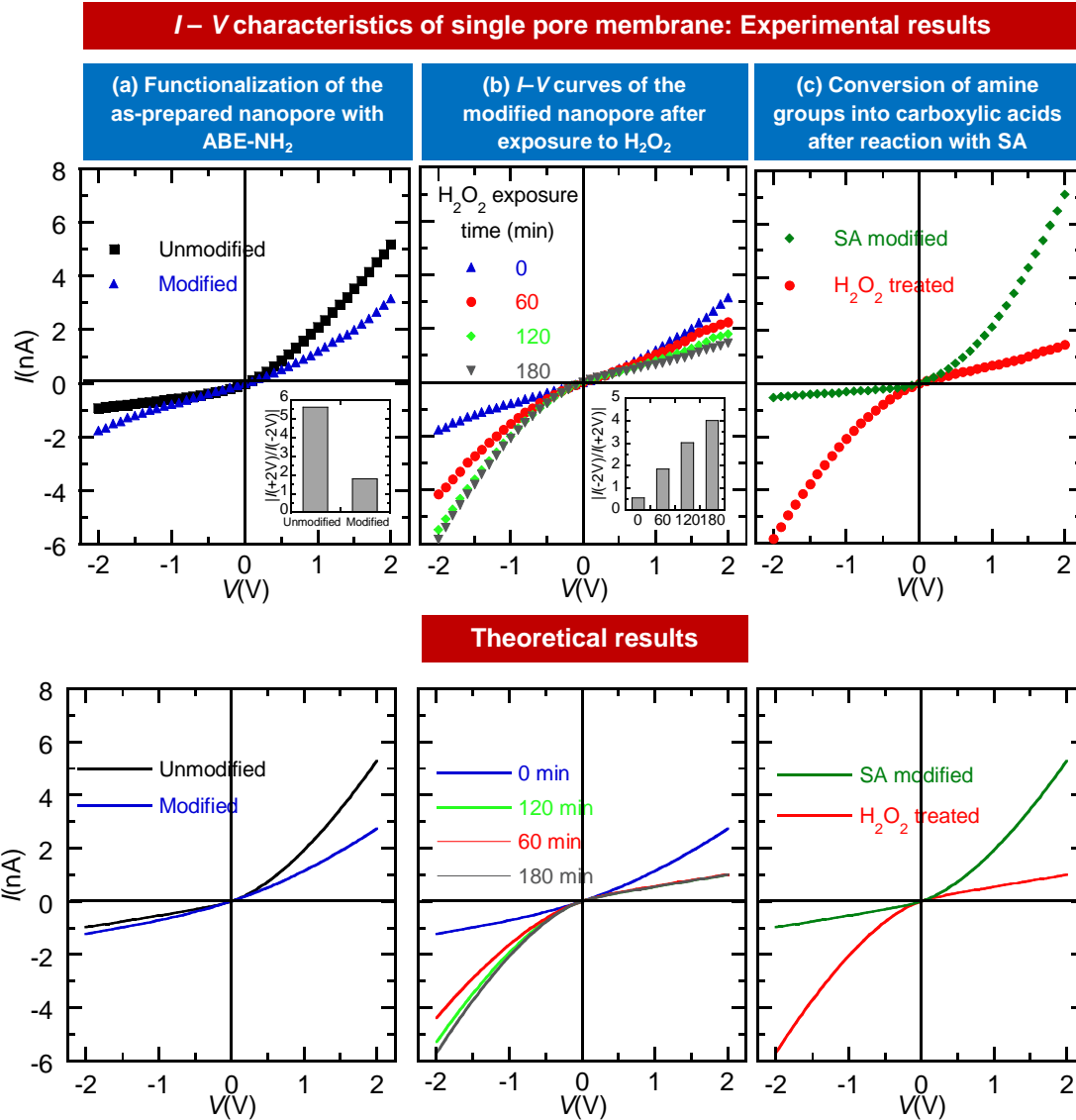


Figure 2 (a) I - V curves of a single asymmetric nanopore with approximate tip and opening diameters $2a_R \sim 25$ nm and $2a_L \sim 600$ nm, respectively, in a 100 mM KCl solution at $pH 5.6 \pm 0.2$. The inset shows the rectification ratios for the same pore prior to (black) and after (blue) chemical modification. (b) I - V curves of the modified nanopore in electrolyte solution before (blue) and after exposure to H_2O_2 for 60 (red), 120 (green) and 180 (black) minutes. The inset shows the rectification ratios as a function of the H_2O_2 exposure time. (c) I - V curves of the H_2O_2 treated nanopore in solution prior to (red) and after (green) reaction with SA. (d)-(f) Theoretical I - V curves obtained from equations (1) and (2) corresponding to the experimental conditions in (a), (b), and (c).

As discussed above, the pore rectification is directly related with the H_2O_2 -dependent surface charge density (Figure 1b-c). The rectification ratio in the inset of Figure 2b, estimated from the corresponding I - V curves, was then regulated by the pore exposition to H_2O_2 . This fact provides a facile tool to correlate the presence of H_2O_2 in solution to the system electronic readout. Indeed, upon exposing the modified pore to the H_2O_2 solution for 60, 120 and 180 min, the electrical

rectification ratio increased to 1.9, 3.0 and 4.0, respectively, to be compared to the unmodified pore value (0.5).

Figure 1c-d shows that the arylboronic ester hydrolysis and subsequent generation of amine groups triggered by H₂O₂ can be further modified through a chemical reaction between the terminal amine groups and succinic anhydride (SA) molecules. When the H₂O₂ treated, aminated pore is exposed to SA, condensation reactions lead to the production of terminal carboxylate groups on the pore surface. After SA modification, the regenerated carboxylate moieties switch the surface charge from positive to negative, changing the pore ionic selectivity and rectification from anionic to cationic (Figure 2c). The carboxylic acid moieties on the SA-modified pore surface suggest the possibility of reusing the pore.

The above experimental results can be described theoretically using a continuous approach based on the Poisson and Nernst-Planck equations,²²⁻²⁶

$$\nabla^2 \phi = -\frac{F}{\varepsilon} \sum_i z_i c_i \quad (1)$$

$$\nabla \cdot \vec{J}_i = -\nabla \cdot \left[D_i \left(\nabla c_i + z_i c_i \frac{F}{RT} \nabla \phi \right) \right] = 0 \quad (2)$$

where $c_i(x)$, z_i , \vec{J}_i , and D_i are the local concentration, charge number, flux density, and diffusion coefficient of ion i , respectively, with $\phi(x)$ being the local electric potential and ε the electrical permittivity. In equation (2), T is the absolute temperature, with F and R being the Faraday and universal gas constants, respectively. The pore radius at a point of coordinate x along the pore axis is described by the equation

$$a(x) = \frac{a_R - a_L \exp[-(d/h)^n] - (a_R - a_L) \exp[-(x/d)^n (d/h)^n]}{1 - \exp[-(d/h)^n]} \quad (3)$$

where d is the pore length and parameters n and d/h control the pore shape.²⁴ Equations (1)-(3) can be integrated numerically to give the ionic flux densities, and then the total electric current I through the nanopore, at each applied voltage V (see references 22 and 26 for details). The above model is useful to describe the I - V curves of different nanopores²²⁻²⁶ using a reduced number of fitting parameters. Figure 2d-f shows that this is also the case of the present experimental results. The best fitting between theory and experiments has been found using $d/h = 0$ and $n = 1.25$ in the calculations, which gives a pore profile with a convex tip,²⁴ slightly deviated from a perfect

conical shape. Once the pore shape has been determined, the only free parameter in the theoretical curves is the surface charge density σ (in units e/nm^2 , where e is the elementary charge). The values of σ used in the calculations were -0.3 , -0.06 , (Figure 2d, unmodified and modified pore, respectively), -0.06 , $+0.2$, $+0.28$ and $+0.35$ (Figure 2e, 0 min, 60 min, 120 min and 180 min of H_2O_2 exposure, respectively), and -0.3 and $+0.35$ (Figure 2f, SA modified and H_2O_2 treated pore, respectively). These values are reasonable, as shown previously with these types of pores.^{22,24}

Finally, Figure 3a-c shows the I - V curves of a multipore membrane containing $\sim 10^4$ asymmetric pores/ cm^2 approximately. This membrane was etched along with the same single-pore membrane used in the functionalizations discussed above. The experimental results suggested that the ionic transport across the multipore membrane can be controlled using similar conditions to those of the single-pore membrane (Figures 2a-c). Indeed, the I - V curves of Figure 3a reveal that the number of open pores contributing to the electric current was approximately $2 \times 10^3/\text{cm}^2$. The surface functionalization method developed for the single-pore membrane can then be integrated and exploited in multipore nanofluidic devices. The scalability characteristics should be useful for practical applications. Figure 3d-f shows that the theoretical curves can reproduce the experimental trends observed assuming the same pore shape as in the single pore experiments, with σ (in e/nm^2) = -0.3 and -0.06 (Figure 3d, unmodified and modified pore, respectively), -0.06 , $+0.02$, $+0.07$ and $+0.08$ (Figure 3e, 0 min, 60 min, 120 min and 180 min of H_2O_2 exposure, respectively), and -0.06 and $+0.08$ (Figure 3f, SA modified and H_2O_2 treated pore, respectively). Note that the experiments in Figure 3b show that the negative currents after the H_2O_2 exposure were slightly lower (in absolute value) than the positive currents characteristic of the as prepared pore (Figure 3a). This is not the case for the single pore sample in Figure 2, where these negative currents in Figure 2b were slightly higher than those characteristic of the as-prepared pore in Figure 2a. As a result, the values of σ found for the multipore membrane are significantly lower than those found for the single pore sample.

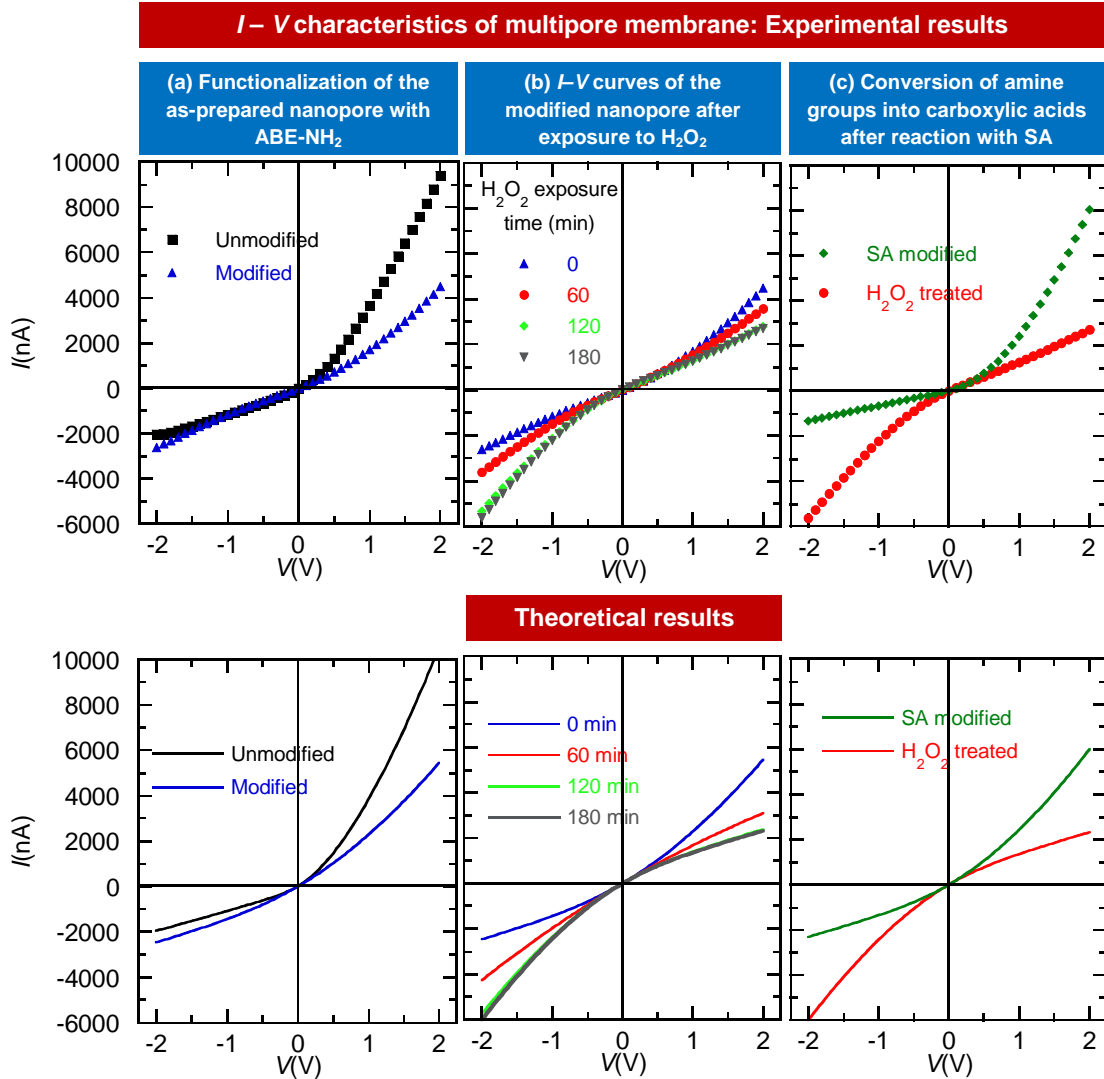


Figure 3. (a) I – V curves of a multipore membrane with 10^4 asymmetric pores/cm² prior to (black) and after (blue) modification with BEC-NH₂ groups. (b) I – V curves of a modified multipore membrane before (blue) and after exposition to a H₂O₂ solution for a period of 60 (red), 120 (green) and 180 (black) min. (c) I – V curves of a H₂O₂ treated multipore membrane prior to (red) and after (green) reaction with SA. All measurements were carried out in a non-buffered 100 mM KCl solution at $pH\ 5.6 \pm 0.2$. (d)–(f) Theoretical I – V curves obtained from equations (1) and (2) corresponding to the experimental conditions in (a), (b), and (c).

In summary, we have described the reversible chemical functionalization of H₂O₂-sensitive asymmetric nanopores, showing experimentally and theoretically that the I – V curves provide a suitable method to monitor the solution properties from electronic readouts. Also, we have demonstrated the scalability of the single pore characteristics to a multipore membrane whose output could be readily controlled, a crucial step to useful nanofluidic devices.

References

- (1) Barnham, K. J.; Masters, C. L.; Bush, A. I. *Nat. Rev. Drug Discovery* **2004**, *3*, 205.
- (2) Dickinson, B. C.; Chang, C. J. *J. Am. Chem. Soc.* **2008**, *130*, 9638.
- (3) Finkel, T.; Serrano, M.; Blasco, M. A. *Nature* **2007**, *448*, 767.
- (4) Jin, H.; Heller, D. A.; Kalbacova, M.; Kim, J. H.; Zhang, J. Q.; Boghossian, A. A.; Maheshri, N.; Strano, M. S. *Nat. Nanotechnol.* **2010**, *5*, 302.
- (5) Lin, M. T.; Beal, M. F. *Nature* **2006**, *443*, 787.
- (6) Dickinson, B. C.; Huynh, C.; Chang, C. J. *J. Am. Chem. Soc.* **2010**, *132*, 5906.
- (7) Chen, W. W.; Li, B. X.; Xu, C. L.; Wang, L. *Biosensor. Bioelectron.* **2009**, *24*, 2534.
- (8) Tahirovic, A.; Copra, A.; Omanovic-Miklicanin, E.; Kalcher, K. *Talanta* **2007**, *72*, 1378.
- (9) Bustos, E. B.; Chapman, T. W.; Rodriguez-Valadez, F.; Godinez, L. A. *Electroanalysis* **2006**, *18*, 2092.
- (10) Kausaite-Minkstimiene, A.; Mazeiko, V.; Ramanaviciene, A.; Ramanavicius, A. *Biosens. Bioelectron.* **2010**, *26*, 790.
- (11) Ali, M.; Tahir, M. N.; Siwy, Z.; Neumann, R.; Tremel, W.; Ensinger, W. *Anal. Chem.* **2011**, *83*, 1673.
- (12) Apel, P. Y.; Korchev, Y. E.; Siwy, Z.; Spohr, R.; Yoshida, M. *Nucl. Instrum. Methods Phys. Res., Sect. B* **2001**, *184*, 337.
- (13) Ali, M.; Ramirez, P.; Mafe, S.; Neumann, R.; Ensinger, W. *ACS Nano* **2009**, *3*, 603.
- (14) Filippis, A. d.; Morin, C.; Thimon, C. *Synth. Commun.* **2002**, *32*, 2669.
- (15) Broaders, K. E.; Grandhe, S.; Fréchet, J. M. J. *J. Am. Chem. Soc.* **2011**, *133*, 756.
- (16) Ali, M.; Nasir, S.; Ramirez, P.; Ahmed, I.; Nguyen, Q. H.; Fruk, L.; Mafe, S.; Ensinger, W. *Adv. Funct. Mater.* **2012**, *22*, 390.
- (17) Vlassioug, I.; Siwy, Z. S. *Nano Lett.* **2007**, *7*, 552.
- (18) Guo, W.; Tian, Y.; Jiang, L. *Acc. Chem. Res.* **2013**, *46*, 2834.
- (19) Siwy, Z. S. *Adv. Funct. Mater.* **2006**, *16*, 735.
- (20) Kuivila, H. G.; Armour, A. G. *J. Am. Chem. Soc.* **1957**, *79*, 5659.
- (21) Lo, L.-C.; Chu, C.-Y. *Chem. Commun.* **2003**, 2728.
- (22) Cervera, J.; Schiedt, B.; Neumann, R.; Mafe, S.; Ramirez, P. *J. Chem. Phys.* **2006**, *124*, 104706.
- (23) Nasir, S.; Ramirez, P.; Ali, M.; Ahmed, I.; Fruk, L.; Mafe, S.; Ensinger, W. *J. Chem. Phys.* **2013**, *138*, 034709.
- (24) Ramirez, P.; Apel, P. Y.; Cervera, J.; Mafe, S. *Nanotechnology* **2008**, *19*, 315707.
- (25) Ramirez, P.; Cervera, J.; Ali, M.; Ensinger, W.; Mafe, S. *ChemElectroChem* **2014**, *1*, 698.
- (26) Ramirez, P.; Gomez, V.; Ali, M.; Ensinger, W.; Mafe, S. *Electrochem. Commun.* **2013**, *31*, 137.